

IONIC MASS TRANSFER IN FLOWING SOLUTIONS. ELECTROCHEMICAL REACTIONS UNDER IONIC MASS-TRANSFER RATE CONTROL ON CYLINDRICAL ELECTRODES*

J. C. BAZÁN and A. J. ARVÍA

Instituto Superior de Investigaciones, Facultad de Química y Farmacia, and
División Ingeniería Química, Facultad de Ciencias Fisicomatemáticas, Universidad de
La Plata, La Plata, Argentina

Abstract—Several electrochemical reactions under ionic mass-transfer rate-control have been studied on cylindrical electrodes forming part of electrolysis cell. The electrodeposition of copper and the redox reactions for the ferro-ferricyanide systems have been examined, in each case with a large excess of a suitable inert electrolyte. The influences of concentration of the reacting species, rate of flowing, viscosity and diffusivity, height of the working electrode, temperature, and distance between anode and cathode, were studied under streamline-flow conditions. The data are fitted by the dimensionless equation

$$Sh = 0.525 \cdot eR_d^{1/2} \cdot Sc^{1/3} \cdot \left(\frac{h}{d}\right)^{3/4}$$

The temperature dependence of the kinetic constant yielded the following experimental heats of activation (a) for copper ion deposition 4800 ± 200 cal/mole (b) for ferricyanide reduction, 3400 ± 200 cal/mole (c) for ferrocyanide oxidation, 3700 ± 200 cal/mole

Since the kinetic constant increases when the flow rate is increased and also when the electrode height is decreased, a departure from reversibility has been observed for the redox system reaction when suitable experimental conditions are chosen.

Résumé—On a étudié la vitesse du transport de masse pour le cas d'électrodes cylindriques concentriques, le liquide coulant à travers l'espace compris entre les deux cylindres. On a utilisé diverses réactions d'électrode: Réduction du cuivre, oxydation du ferrocyanure, réduction du ferricyanure. Les paramètres suivants ont été variés: Vitesse d'écoulement de l'électrolyte, concentration et viscosité de la solution, hauteur et diamètre des électrodes cylindriques ainsi que la température. Les résultats peuvent être exprimés à l'aide de la corrélation sans dimensions

$$Sh = 0,525 \cdot Re_d^{1/2} \cdot Sc^{1/3} \cdot \left(\frac{h}{d}\right)^{3/4}$$

La variation de la vitesse de transport avec la température correspond à une énergie d'activation de (a) 4800 ± 200 cal/mol pour la réduction du cuivre, (b) 3400 ± 200 pour la réduction du ferricyanure et (c) 3700 ± 200 pour l'oxydation du ferrocyanure. Comme la vitesse du transport massique augmente lorsque l'écoulement du liquide devient plus rapide et lorsque hauteur diminue on peut observer, dans certaines conditions, des écarts de la réversibilité pour le système redox étudié.

Zusammenfassung—Es wurde die Geschwindigkeit des elektrolytischen Stofftransports an konzentrischen zylindrischen Elektroden untersucht, wobei der Elektrolyt durch den Raum zwischen den Zylindern strömte. Es wurden dabei verschiedene Elektrodenreaktionen verwendet: Kupferabscheidung, Oxydation von Ferrocyanid, Reduktion von Ferricyanid. Variiert wurden: die Durchflussgeschwindigkeit, die Konzentration und die Zähigkeit der Lösung, die Höhe und der Durchmesser der zylindrischen Elektroden sowie die Temperatur. Die Ergebnisse können durch folgende dimensionslose Korrelation ausgedrückt werden:

$$Sh = 0.525 \cdot Re_d^{1/2} \cdot Sc^{1/3} \cdot \left(\frac{h}{d}\right)^{3/4}$$

Der Temperaturkoeffizient der Stoffübergangszahl entspricht einer Aktivierungswärme von (a) 4800 ± 200 kal/Mol. für die Kupferabscheidung, (b) 3400 ± 200 für die Ferricyanidreduktion und

* Manuscript received 18 June 1963.

(c) 3700 ± 200 für die Ferrocyanidoxydation. Da die Geschwindigkeit des Stofftransports mit zunehmender Strömungsgeschwindigkeit und abnehmender Höhe grösser wird, können unter gewissen Bedingungen Abweichungen von der Reversibilität bei den untersuchten Redoxvorgängen beobachtet werden.

INTRODUCTION

In a previous paper¹ we examined an ionic mass-transfer process by electrolysis of copper-sulphate-sulphuric-acid solutions on annular cathodes of different sizes. The results could be correlated in a relatively simple dimensionless equation, and indicated that with streamlined flow, the mass transfer could be considered as taking place on a vertical flat plate with streamline flow along it, the hydrodynamic and diffusion boundary layers having merged. The counter-electrode has no appreciable effect on the profile of the working electrode.

Those results led us to study ionic mass-transfer controlled reactions on inner cylindrical electrodes of a concentric tubular cell, vertically placed. Mass transfer under those conditions has been studied by Putnam *et al.*² for an electrolysis cell of fixed size. Our previous experience, however, suggested that a fuller study of this problem, with change of the available physicochemical and geometrical variables, would be of interest to obtain the ionic mass-transfer rate equation, and to compare the results with those previously obtained.

Two different types of reactions have been investigated, one in which there is a continuous change of the electrode surface and another involving redox reactions with soluble species respectively the electrodeposition of copper and the redox reactions of ferro-ferricyanide solutions.

The rate equations indicate that both the flow velocity and the height of the working electrode could be adjusted to increase the rate of the diffusion process and therefore, under certain conditions departures from reversibility can be observed in otherwise reversible electrode reactions.

From this fact arises the possibility of using tubular cell arrangements in hydrodynamic voltammetry. This application will be considered in a future publication.

EXPERIMENTAL

1. The electrolysis cell

The electrolysis cell was made with a nickel-plated stainless-steel tube or with a copper tube which was at the same time the non-polarizable electrode of the cell and a part of the hydrodynamic circuit.

Copper and nickel non-polarizable electrodes of diameter of 1.90 and 2.13 cm respectively were used.

The nickel-plated electrode was especially suitable when alkaline solutions of potassium ferro- and ferricyanide were used, whereas the copper tube was employed with acid copper sulphate solutions.

Working electrodes were made of pure nickel rods, copper plated when used for the electrodeposition of copper.

A diagram of the cell is shown in Fig. 1. A set of seven working electrodes was used, with the dimensions given in Table 1.

The cylindrical working electrode was axially held into the cell by means of Lucite rods of the same diameter. The cylindrical metallic pieces were screwed and stuck into cylindrical rods of Lucite and the whole arrangement was finished to the proper diameter and polished on a lathe. Solutions flowed through the annular space formed

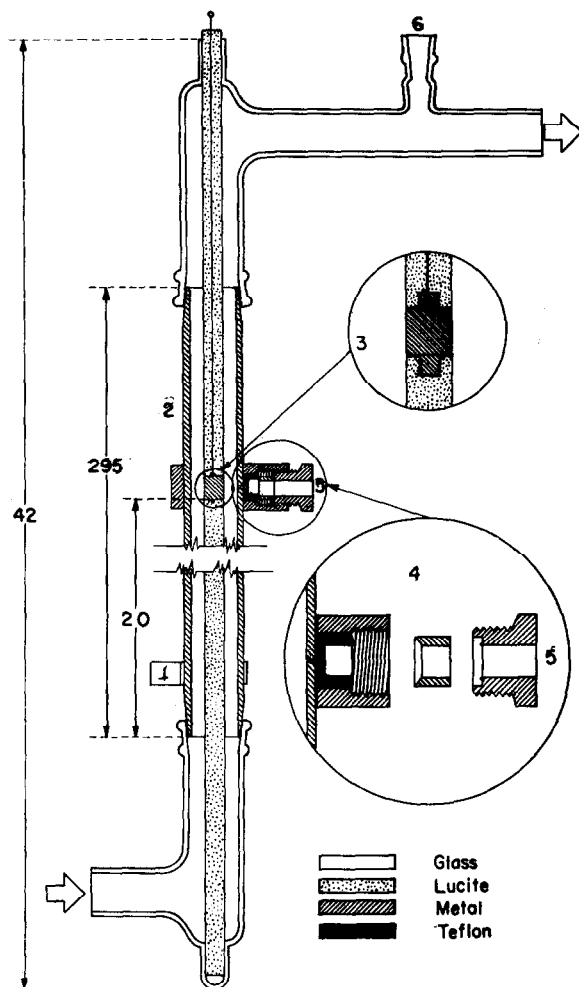


FIG. 1. Electrolysis cell.

1. electrical contact.
2. counter electrode.
3. detail of working electrode.
4. detail of reference electrode joint.
5. to reference electrode.
6. temperature control.

Lengths in cm.

TABLE I

Electrode	h cm	ϕ cm	A cm ²	d cm
1	1.05	1.00	3.30	1.88
2	4.00	1.00	12.6	1.88
3	0.20	1.00	0.628	1.88
4	0.80	1.00	2.51	1.88
5	0.80	1.30	3.27	1.69
6	0.80	0.65	1.63	2.03
7	0.08	1.00	0.215	1.88

by the non-polarizable electrode and the insulating rod through a distance of about 30 cm long before reaching the edge of the working electrode, the actual site where the electrochemical process under diffusion control began to occur. The total length of the electrolytic cell was 47 cm.

The reference electrode was made with platinum wire, copper plated when necessary and immersed in the same solution employed in the cell. It was attached to the external electrode by means of a special metallic holder and the solution was in contact with the flowing liquid through a capillary tube and a pin hole opened on the electrode wall. The reference electrode capillary tip was fixed in the proper position with the aid of Teflon gaskets. It was placed just in front of the middle height of the inner electrode, avoiding any disturbances on the flowing solution.

The rest of the cell was made of Pyrex glass tubing and assembled by means of standard tapered glass joints.

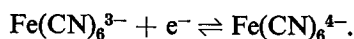
Temperature was read on a calibrated mercury thermometer in the solution immediately beyond the cell.

2. Flowing solutions

Two different solutions were studied. The first was an equimolecular solution of potassium ferrocyanide and ferricyanide in nearly 2 M sodium hydroxide. The concentrations of the reacting species were varied from 0.008 to 0.1 M. These solutions were suitable to study the diffusion process with a reaction where soluble species were involved. For the present case, nickel electrodes were the most suitable.

This redox system has no appreciable activation polarization on nickel electrodes if these are cathodically activated by a hydrogen evolution treatment before assembling the cell.³ This was done by placing them in 5% sodium hydroxide solution at a cathode current density of *ca* 20 mA/cm².

The cell had a large surface ratio between the working and the non-polarizable electrodes, making possible independent study of the cathodic and anodic reactions by changing the electrode polarity. The cathodic and anodic reactions are



The second system was a solution of copper sulphate in 1.5 M sulphuric acid. The copper ion concentration was varied from 0.008 to 0.223 M. Glycerol was added to the copper-sulphate-sulphuric acid-solutions in order to have a range of viscosities from 1.078×10^{-2} to 6.130×10^{-2} cm²/s. The solution was circulated continuously through the cell. Further experimental details and a description of the rest of the arrangement, electrical measuring devices and the procedure are given in our previous publication.¹

Temperature was varied between 25 and 45°C, and the flow velocity from 6 to 50 cm/s.

Purified nitrogen was bubbled continuously during each experiment to eliminate most of the dissolved oxygen, as before.

RESULTS AND INTERPRETATION

Typical polarization curves obtained under different conditions are shown in Figs. 2-5.

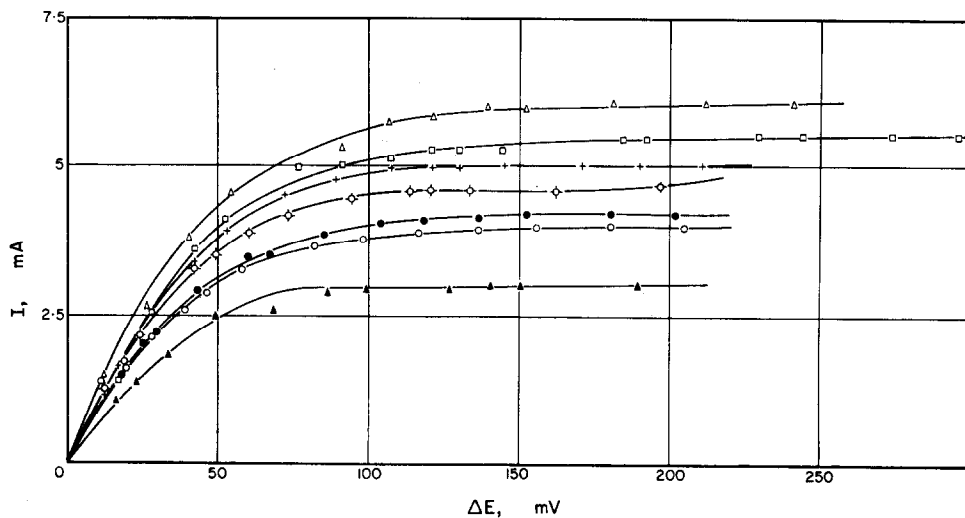


FIG. 2. Current/voltage curves.
 Electrode 1. 25°C. $C_{o,3}$, 0.0111 M.
 ●: 22.0; ○: 27.5; ×: 32.3;
 □: 35.9; △: 38.9; ▲: 6.4; ○: 18.5 cm/s

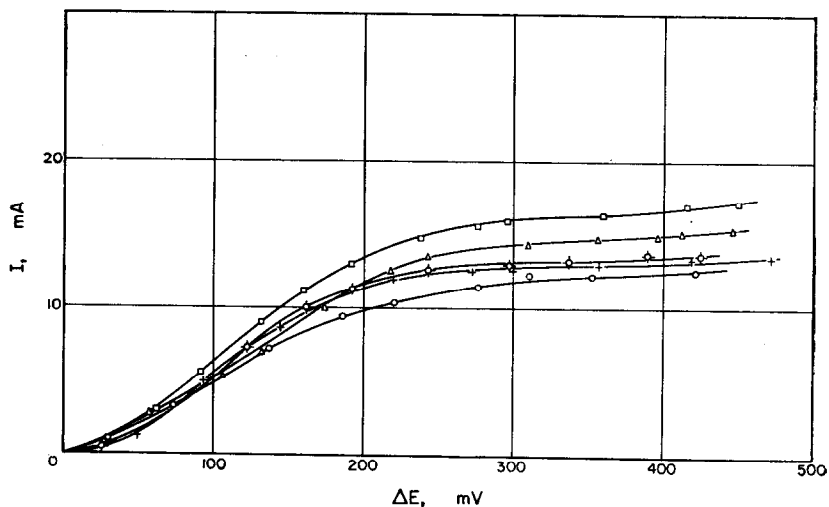


FIG. 3. Current/voltage curves.
 Electrode 1. 25°C. C_o , 0.0480 M; C_g , 5.71 M;
 ○: 8.4; +: 20.0; ○: 24.8;
 △: 30.4; □: 37.8 cm/s

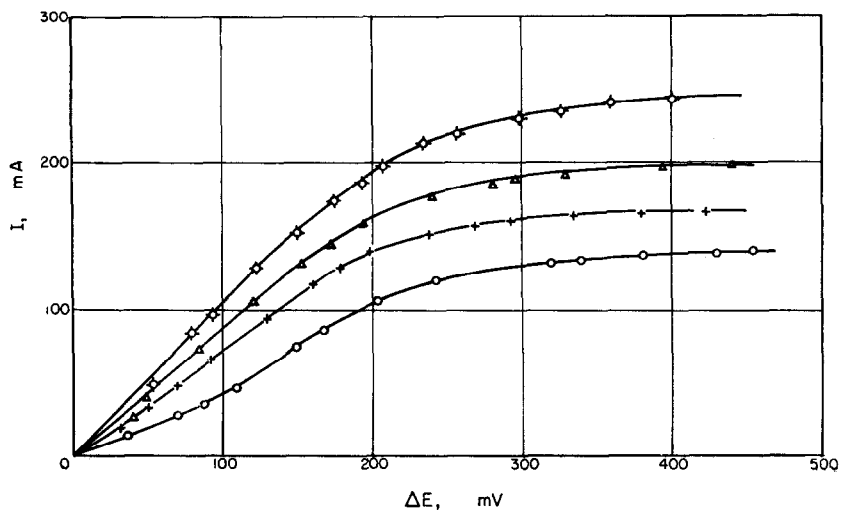


FIG. 4. Current/voltage curves.

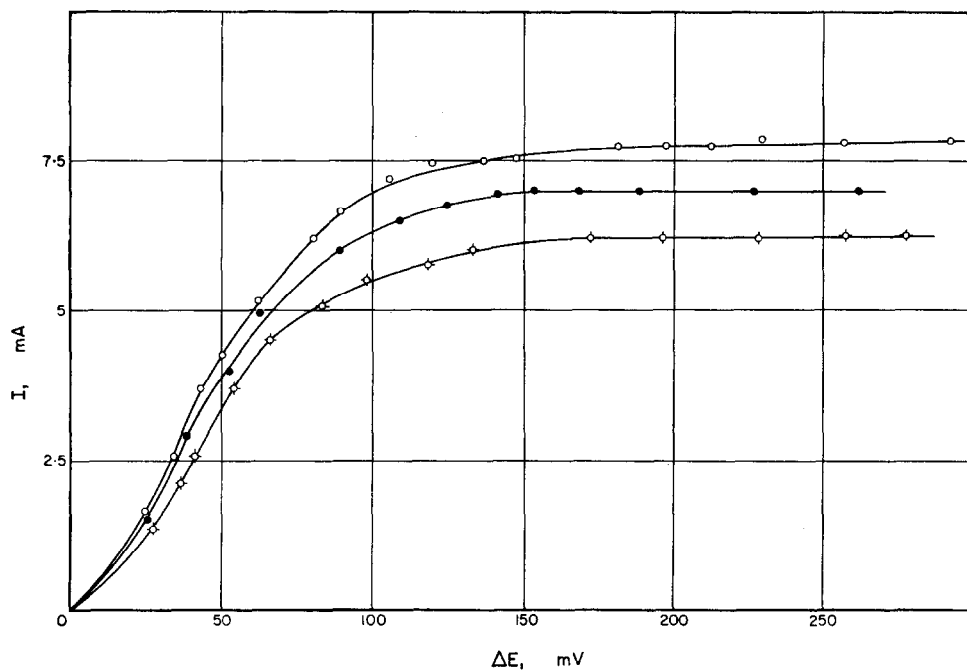
Electrode 2. 25°C. C_0 , 0.0472 M; Δ : 37.8; \circ : 20.0; +: 26.0; \circ -: 51.7 cm/s

FIG. 5. Current/voltage curves.

Electrode 1. 25°C. $C_{0,3}$, 0.0113 M. \circ : 38.5; \bullet : 33.1; \circ -: 23.9 cm/s

Experimental data are given in Tables 2-6. The following nomenclature is used:

Nr is the run number; V is the linear mean velocity of the flowing solution in cm/s, calculated from the total flux and the area of the annular section of the cell; i_L is the limiting current density in mA/cm²; k is the mass-transfer kinetic constant in cm/s, calculated from the current density and the concentration of the diffusing species; C_o , C_a , C_g , $C_{o,3}$, $C_{o,4}$ and C_h refer to copper ion, sulphuric acid, glycerol, ferricyanide ion, ferrocyanide ion and sodium hydroxide concentrations respectively, in mol/l; h , ϕ and d are the height, diameter and equivalent diameter of the working electrode in cm; ν and D are the average kinematic viscosity and diffusion coefficient of the reacting species, both in cm²/s; ΔC_a and ΔC_h are the changes of concentrations of the supporting electrolytes in mol/l; Sh , Sc and Re are the Sherwood, Schmidt and Reynolds numbers respectively. The experimental data shown in the Tables are for 25°C.

From the temperature dependence of the kinetic constant shown in Figs. 6 and 7, the experimental temperature coefficients were obtained. The corresponding heats of activation for the different processes are as follows: for copper ion deposition, 4800 ± 200 cal/mol; for ferricyanide ion reduction, 3400 ± 200 cal/mol; and for ferrocyanide ion oxidation, 3700 ± 200 cal/mol.

TABLE 2. ELECTRODE 1

Nr	V cm/s	i_L mA/cm ²	$k \times 10^3$	Sh	Re_d	$Re_d^{1/3} \cdot Sc^{1/3} \cdot \left(\frac{h}{d}\right)^{3/4}$
$C_{o,4}$: 0.0111 M; $C_{o,3}$: 0.0113 M; C_h : 2.030 M; ΔC_h : 0.004 M; D : 5.00×10^{-6} cm ² /s; ν : 1.39×10^{-2} cm ² /s; Sc : 2790.						
A-18	6.41	0.97	0.91	199	864	269
19	18.4	1.16	1.08	237	2490	455
20	24.5	1.25	1.17	256	3300	505
21	28.3	1.36	1.27	277	3820	563
22	33.1	1.51	1.41	308	4450	608
23	35.9	1.58	1.47	323	4845	635
24	38.5	1.75	1.63	357	5200	658
25	41.4	1.80	1.68	370	5600	682
C-15	18.4	1.20	1.10	220	2490	455
16	22.0	1.26	1.15	231	2965	502
17	27.5	1.37	1.26	253	3715	561
18	32.3	1.50	1.38	278	4345	604
19	35.9	1.57	1.44	292	4830	635
20	38.9	1.80	1.65	332	5250	662
21	6.41	0.90	0.83	163	864	267
$C_{o,4}$: 0.1145 M; $C_{o,3}$: 0.0930 M; C_h : 2.070 M; ΔC_h : 0.042 M; D : 4.72×10^{-6} cm ² /s; ν : 1.500×10^{-2} cm ² /s; Sc : 3110.						
A-52	6.44	8.72	0.79	191	806	270
53	10.3	10.3	0.94	226	1332	348
54	13.7	11.4	1.04	251	1710	394
55	20.0	12.9	1.16	282	2506	477
56	24.0	14.0	1.27	306	3095	523
C-46	23.3	12.3	1.38	306	2920	512
47	20.0	11.5	1.28	285	2506	477
48	13.7	9.94	1.11	246	1710	394
49	10.6	9.09	1.10	225	1332	348
50	6.44	7.21	0.80	178	806	270

TABLE 3. ELECTRODE 1

Nr	V cm/s	i_L mA/cm ²	$k \times 10^3$	Sh	Re _a	Re _a ^{1/3} · Sc ^{1/3} · $\left(\frac{h}{d}\right)^{3/4}$
C _o : 0.0086 M; C _a : 1.471 M; ΔC _a : 0.004 M; D: 6.34 × 10 ⁻⁶ cm ² /s; ν: 1.067 × 10 ⁻² cm ² /s; Sc: 1684						
Cu-54	12.2	2.42	1.46	242	1846	309
55	8.30	1.88	1.14	188	1256	256
56	9.17	1.92	1.16	192	1388	282
57	16.4	2.61	1.54	260	2490	360
58	30.2	3.15	1.90	315	4580	487
59	20.1	2.69	1.62	270	3047	397
C _o : 0.2230 M; ΔC _a : 1.411 M; C _a : 0.095 M; D: 6.25 × 10 ⁻⁶ cm ² /s; ν: 1.2140 × 10 ⁻² cm ² /s; Sc: 1945						
Cu-60	8.30	46.7	1.08	183	1103	252
61	9.17	49.4	1.15	193	1218	264
62	12.2	56.9	1.32	223	1622	304
63	16.4	62.7	1.46	245	2185	353
64	30.2	83.1	1.93	324	4025	480
65	20.1	75.7	1.76	296	2678	392
C _o : 0.0472 M; C _a : 1.420 M; ΔC _a : 0.021 M; D: 6.25 × 10 ⁻⁶ cm ² /s; ν: 1.088 × 10 ⁻² cm ² /s; Sc: 1596						
Cu-11	20.0	13.3	1.45	244	3000	398
12	37.6	17.7	1.95	327	5635	545
13	51.3	20.3	2.22	374	7700	640
14	28.6	15.5	1.70	286	4280	475
C _o : 0.0445 M; C _a : 1.500 M; C _o : 3.11 M; ΔC _a : 0.008 M; D: 2.85 × 10 ⁻⁶ cm ² /s; ν: 2.887 × 10 ⁻² cm ² /s; Sc: 10120						
Cu-33	20.0	6.52	0.76	280	1117	437
34	28.6	7.12	0.83	306	1598	477
35	37.7	7.88	0.92	338	2105	550
36	51.7	8.80	1.02	378	2891	704
C _o : 0.0480 M; C _a : 1.470 M; C _o : 5.71 M; ΔC _a : 0.006 M; D: 1.45 × 10 ⁻⁶ cm ² /s; ν: 6.130 × 10 ⁻² cm ² /s; Sc: 42180						
Cu-44	20.0	4.03	0.435	314	526	484
45	24.7	4.30	0.464	335	648	536
46	30.4	4.48	0.483	350	800	595
47	37.7	4.94	0.533	385	995	665

The experiments clearly show that the limiting current density is linearly related to the concentration of the reacting ion as found earlier for annular electrodes.

A general equation for the variables involved in the present study may be expected to be dimensionless, of the form

$$Sh = K \cdot Sc^a \cdot Re^b, \quad (1)$$

as obtained for the tubular electrolysis cell.¹ In this case the dimensionless numbers are defined as

$$Sh = \frac{k \cdot X}{D}, \quad Sc = \frac{\nu}{D}, \quad Re = \frac{VX}{\nu},$$

where X is a characteristic length, in cm, chosen according to different criteria analysed later, and K , a and b are constants to be determined experimentally.

A linear relationship was found between the kinetic constant and the square root

TABLE 4. ELECTRODE 2

<i>Nr</i>	<i>V</i> cm/s	<i>i_L</i> mA/cm ²	<i>k</i> × 10 ⁸	<i>Sh</i>	<i>Re_d</i>	<i>Re_d^{1/2} · Sc^{1/3} · (h/d)^{3/4}</i>
<i>C_{o,4}</i> : 0.0111 M; <i>C_{o,8}</i> : 0.0113 M; <i>C_h</i> : 2.030 M; ΔC_h : 0.004 M; <i>D</i> : 5.00×10^{-6} cm ² /s; ν : 1.394×10^{-2} cm ² /s; <i>Sc</i> : 2790						
A-32	16.5	0.80	0.74	616	2230	1182
33	23.9	0.99	0.92	770	3320	1422
34	28.3	1.07	1.00	837	3820	1550
35	33.1	1.12	1.04	865	4450	1670
36	38.5	1.23	1.15	957	5195	1810
37	41.4	1.29	1.20	1000	5600	1870
38	47.5	1.34	1.25	1044	6410	2007
C-28	47.5	1.22	1.12	868	6410	2007
29	41.4	1.14	1.04	808	5600	1870
30	38.5	1.08	0.99	752	5195	1810
31	33.1	0.98	0.90	687	4450	1670
<i>C_{o,4}</i> : 0.1145 M; <i>C_{o,8}</i> : 0.0930 M; <i>C_h</i> : 2.070 M; ΔC_h : 0.042 M; <i>D</i> : 4.72×10^{-6} cm ² /s; ν : 1.500×10^{-2} cm ² /s; <i>Sc</i> : 3110						
A-70	10.6	7.15	0.65	597	1332	960
71	13.7	7.88	0.72	656	1710	1088
72	20.0	9.40	0.81	754	2506	1315
C-65	20.0	7.65	0.85	723	2506	1315
66	13.7	6.71	0.75	634	1710	1088
67	10.6	6.07	0.68	575	1332	960
<i>C_o</i> : 0.0472 M; <i>C_a</i> : 1.420 M; ΔC_a : 0.021 M; <i>D</i> : 6.25×10^{-6} cm ² /s; ν : 1.078×10^{-2} cm ² /s; <i>Sc</i> : 1596						
Cu-20	37.6	12.2	1.34	860	5635	1755
21	51.7	14.1	1.55	990	7750	2060
22	58.6	15.3	1.68	1075	8780	2190
23	28.6	10.5	1.16	740	4280	1530
24	20.0	9.17	1.01	645	3000	1280

of the mean flow velocity, as shown in Fig. 8 for the different systems. This shows that the exponent b in (1) is $\frac{1}{2}$.

By fixing the values of V , the relation of the Sherwood number to the Schmidt number was also determined; the results are shown in Fig. 9 as a plot of $\log Sh$ vs $\log Sc$. The wide range of Sc numbers experimentally covered gives sound support to this relationship. The average slope of the straight lines drawn through the experimental point is $\frac{1}{3}$, which is thus the value of exponent a in (1).

The final expression of (1) has been worked out considering two definitions of Reynolds number, taking as characteristic lengths the equivalent diameter of the electrode d , which is the diameter corresponding to the annular section of the cell, and the electrode height, h :

$$Re_d = \frac{V \cdot d}{\nu} \quad \text{and} \quad Re_h = \frac{V \cdot h}{\nu}. \quad (2)$$

A plot of Sh vs $Sc^{1/3} \cdot Re_d^{1/2}$ is presented in Fig. 10; it yields different straight lines according to the height of the corresponding electrode. Therefore, a new dimensionless term including the electrode height has to be added to (1). This has been done by plotting $\log Sh$ as a function of $\log(h/d)$ for fixed values of $Sc^{1/3} \cdot Re_d^{1/2}$, as shown in Fig. 10. The result, shown in Fig. 11, gives $\frac{2}{3}$ for the exponent of the new term of (1).

TABLE 5. ELECTRODE 3

Nr	V cm/s	i_L mA/cm ²	$k \times 10^3$	Sh	Re_d	$Re_d^{1/2} \cdot Sc^{1/3} \cdot \left(\frac{h}{d}\right)^{3/4}$
$C_{o,1}$: 0.0111 M; $C_{o,3}$: 0.0113 M; C_h : 2.030 M; ΔC_h : 0.004 M; D : 5.00×10^{-6} cm ² /s; ν : 1.394×10^{-2} cm ² /s; Sc : 2790						
C-34	18.5	1.59	1.46	56.7	2490	131
35	28.3	1.91	1.75	66.8	3820	173
36	23.1	1.82	1.68	64.0	4450	176
37	38.5	2.04	2.19	83.5	5195	190
38	41.4	2.70	2.48	94.6	5600	198
39	47.5	3.30	3.04	117	6411	213
$C_{o,4}$: 0.1145 M; $C_{o,3}$: 0.0930 M; C_h : 2.070 M; ΔC_h : 0.042 M; D : 4.72×10^{-6} cm ² /s; ν : 1.500×10^{-2} cm ² /s; Sc : 3110						
A-74	20.0	22.3	2.01	92.6	2506	136
75	13.7	19.1	1.73	79.5	1710	113
76	10.6	17.6	1.60	73.5	1332	99.5
C-68	10.6	14.1	1.58	66.8	1332	99.5
69	13.7	15.9	1.77	75.1	1710	113
70	20.0	17.8	1.98	84.1	2506	136
C_o : 0.0472 M; C_a : 1.420 M; ΔC_a : 0.021 M; D : 6.25×10^{-6} cm ² /s; ν : 1.078×10^{-2} cm ² /s; Sc : 1596						
Cu-15	20.0	21.3	2.33	76.6	3000	137
16	28.6	24.8	2.72	87.0	4280	173
17	37.6	29.1	3.20	102	5635	187
18	58.6	36.1	3.96	127	8780	234
19	51.7	34.4	3.77	121	7750	219

Therefore, under the present experimental conditions, the general correlation is

$$Sh = 0.525 Re_d^{1/2} Sc^{1/3} \left(\frac{h}{d}\right)^{3/4}, \quad (3)$$

which is compared with the experimental data in Fig. 12.

The same calculation with the second definition of Reynolds number gives

$$Sh = 0.525 Re_h^{1/2} Sc^{1/3} \left(\frac{h}{d}\right)^{1/4}. \quad (4)$$

Equation (3) gives the following relationships between the formal kinetic constant and the limiting current density and the electrode dimensions and the solution flow properties,

$$k = 0.525 V^{1/2} d^{-1/4} h^{1/4} D^{2/3} \nu^{-1/6}, \quad (5)$$

$$i_L = 0.525 z F C V^{1/2} d^{-1/4} h^{1/4} D^{2/3} \nu^{-1/6}. \quad (6)$$

Nernst's definition of the average thickness of the diffusion layer, δ_N , is

$$\delta_N = 1.90 h^{1/4} d^{1/4} V^{-1/2} D^{1/3} \nu^{1/6}. \quad (7)$$

The *maximum* error in equations (3) and (4), including the errors involved in all the experimental determinations, is 14 per cent, according to the analysis described previously.¹

TABLE 6. ELECTRODES 5, 6 AND 7

$C_{o,4}$: 0.0777 M; $C_{o,3}$: 0.0730 M; C_h : 1.820 M; ΔC_h : 0.029 M; D : 4.84×10^{-6} cm ² /s; ν : 1.479×10^{-3} cm ² /s; Sc : 3053						
Nr	V cm/s	i_L mA/cm ²	$k \times 10^3$	Sh	Re_d	$Re_d^{1/2} Sc^{1/3} \left(\frac{h}{d}\right)^{3/4}$
Electrode 5						
C-80	40.3	14.9	2.11	322	4600	563
81	34.3	13.4	1.91	291	3920	519
82	22.5	11.4	1.61	177	2575	419
A-83	22.5	11.5	1.54	279	2575	419
84	34.3	14.1	1.88	340	3920	519
85	40.3	15.0	2.01	364	4600	563
86	46.8	16.7	2.22	403	5340	606
87	50.4	17.4	2.32	420	5750	529
88	57.8	18.8	2.51	454	6595	673
Electrode 6						
C-83	15.6	9.17	1.30	199	2145	334
84	23.8	11.5	1.63	250	3270	412
85	28.0	12.1	1.72	263	3840	447
86	32.5	12.7	1.82	279	4470	482
87	34.9	13.1	1.85	284	4800	492
88	40.1	13.9	1.97	302	5510	535
A-89	40.1	14.4	1.92	347	5510	535
90	34.9	13.8	1.83	334	4800	492
91	32.5	13.0	1.74	315	4470	482
92	28.0	12.5	1.76	302	3840	447
93	23.8	11.3	1.51	273	3270	412
94	15.6	9.4	1.23	223	2145	334
Electrode 7						
C-89	28.3	23.2	3.27	54.1	3595	81.0
90	38.5	26.3	3.72	61.5	4890	94.4
91	47.5	29.2	4.12	68.1	6027	105
92	54.6	32.2	4.56	75.4	6940	117
93	59.7	32.9	4.66	77.0	7590	123
A-95	28.3	24.6	3.26	53.8	3595	81.0
96	38.5	28.2	3.75	61.9	4890	94.4
97	47.5	30.2	4.01	66.3	6027	105
98	50.6	31.6	4.21	69.4	6430	108
99	54.6	33.6	4.46	73.6	6940	117

For a more detailed treatment of the results, the change of concentration of the supporting electrolyte next to the electrode surface must be also taken into account. It has been evaluated as

$$\Delta C_1 = t_1 \frac{D_2^{2/3}}{D_1^{2/3}} C_2, \quad (8)$$

following from (3), where t_1 is the transport number of species 1.

Values calculated for ΔC_1 are included in the tables. The correction resulting from ΔC_1 affects the diffusion coefficients and viscosity in the electrode region. Nevertheless the fluctuations of these data in the literature are higher than the errors involved in the results.

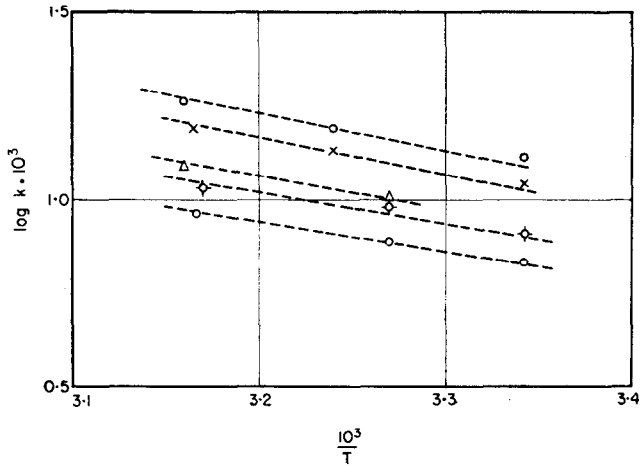


FIG. 6. Arrhenius plot for reduction of ferricyanide ion. (mass-transfer control).

Δ : 20.0; \circ (with electrode 1): 13.7; \circ : 6.4; (with electrode 2):
 \circ : 20.0; \times : 10.6 cm/s;

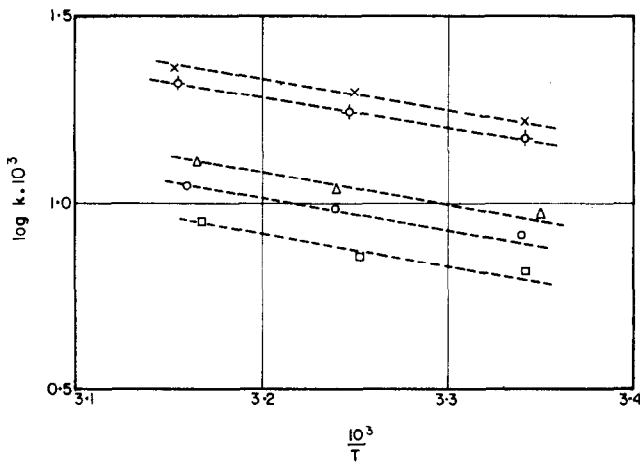


FIG. 7. Arrhenius plot for oxidation of ferrocyanide ion (mass-transfer control).

Δ : 33.3; \circ : 38.5; \square : 10.6; (with electrode 1):
 \circ (with electrode 2): 10.6; \times : 20.0 cm/s

We have also noticed that the maximum uncertainty in the experiments with the potassium-ferrocyanide-ferricyanide-sodium-hydroxide system is in the ionic diffusion coefficient of the reacting species.

DISCUSSION

The experimental equations for the ionic mass-transfer process on the inner cylindrical electrodes of the tubular cell have the form of those found for annular electrodes. As is also the case for the rotating disk electrode,⁵ the conical electrode⁶ in flowing solution, and for the streaming mercury electrode,⁷ k and i_L are functions of the $-1/6$ th power of the kinematic viscosity of the flowing solution and the $2/3$ th power of the diffusion coefficient of the species reacting on the electrode. This type of

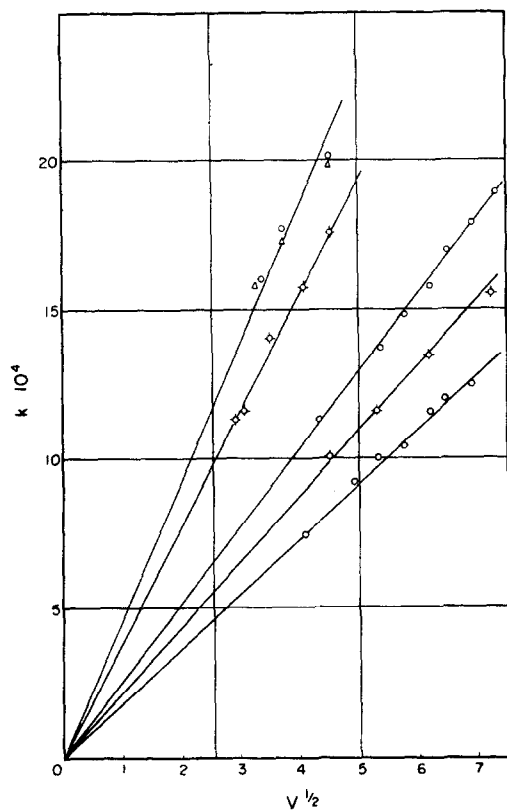


FIG. 8. Plot of k vs $V^{1/2}$.

- \triangle : reduction of ferricyanide ion.
- \circ : oxidation of ferrocyanide ion.
- \ominus : deposition of copper ion.

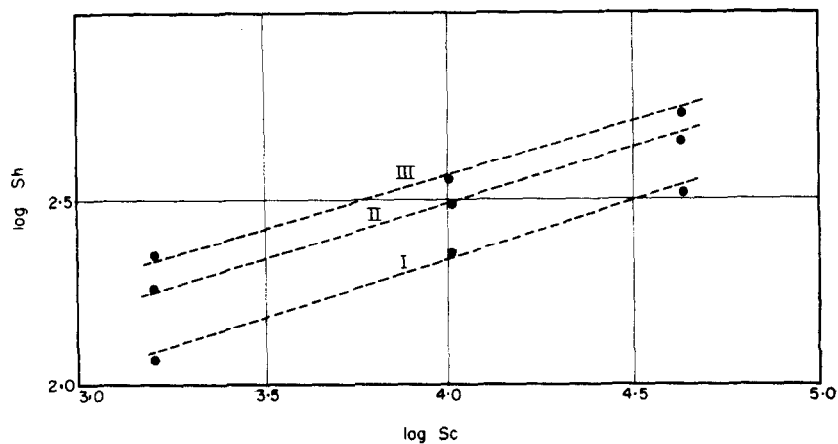


FIG. 9. Plot of $\log Sh$ vs $\log Sc$.

I, $Re_d = 625$; II, $Re_d = 1600$; III, $Re_d = 2500$.

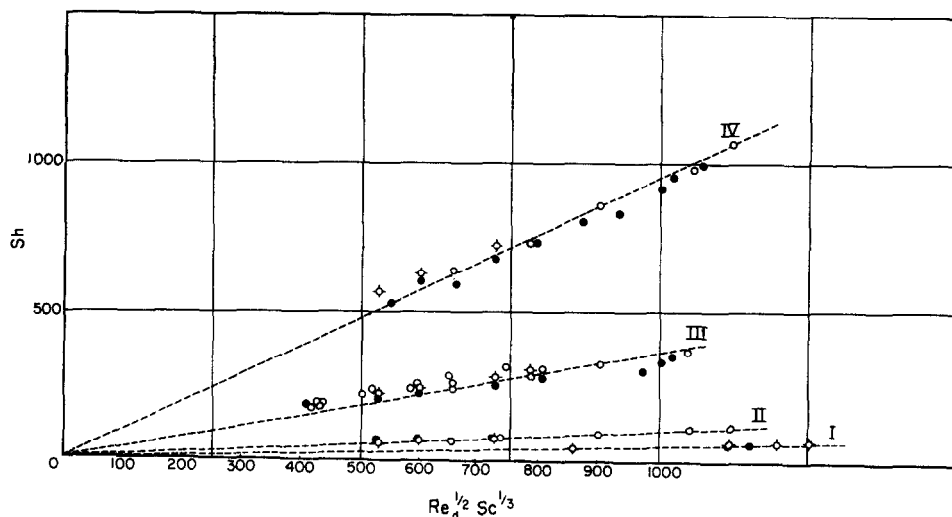


FIG. 10. Plot of Sh vs $Re_a^{1/2} Sc^{1/3}$.

I, electrode 7; II, electrode 3; III, electrode 1; IV electrode 2.

●: oxidation of ferrocyanide ion; ◻: reduction ferricyanide ion;
○: deposition of copper ion.

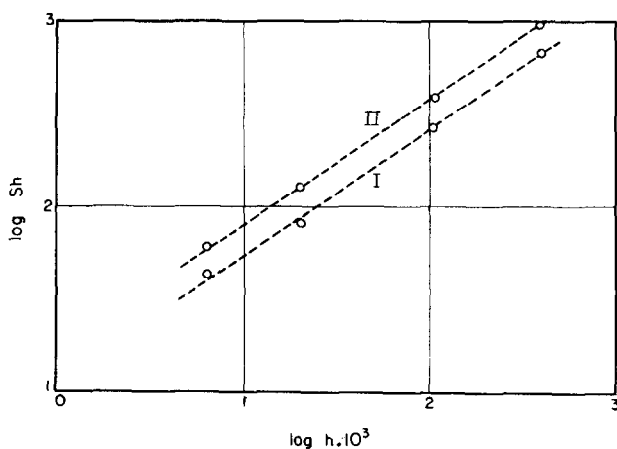


FIG. 11. Plot of $\log Sh$ vs $\log h$.

I, $Re_a^{1/2} Sc^{1/3} = 700$; II, $Re_a^{1/2} Sc^{1/3} = 1000$.

dependence is the one expected when streamline flow occurs on the electrode surface. On the other hand, the ionic mass-transfer mechanism is independent of the electrochemical reactions occurring at the electrodes.

A question arising in the present case concerns the entrance length for a fully developed Poiseuille profile in the annular space. If it is estimated by extending to the present case Schlichting's equation deduced for parallel flat plates, the entrance length would change approximately from 1 to 100 cm, within the flow-rate range of 6–50 cm/s, for distances between electrodes from 0.83 to 1.48 cm and kinematic viscosity from 1×10^{-2} to 7×10^{-2} cm²/s respectively. Therefore, most of the experiments

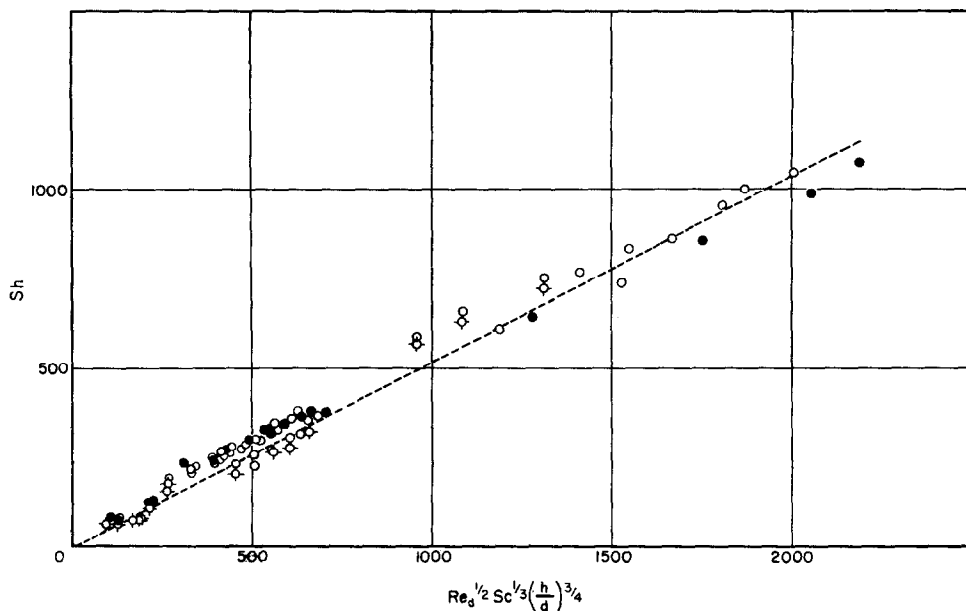


FIG. 12. Plot of equation (3).

●: deposition of copper ion; \ominus : reduction of ferricyanide ion;
○: oxidation of ferrocyanide ion.

correspond to a fully developed hydrodynamic profile whereas some of those at the highest rates employed involve a diffusion process taking place within the region of the entrance length.

Nevertheless, the experimental equations found in the present case agree with the concept of a fully developed hydrodynamic profile having been set up when the diffusion process takes place on the electrode. Certainly the situation is much more complicated than that in the case of parallel flat plates, but in spite of this we conclude that the analysis of the mass-transfer process is approximated by the solutions worked out for flat plate electrodes.

If the hydrodynamic boundary layer is not fully developed, one would more reasonably expect an equation of the L ev eque type⁸ to represent the results. L ev eque's equation predicts a linear dependence of k on the cube root of the flow rate. This was not found in the present work.

When equations (3) and (4) are compared to the one previously found for the annular electrode, the existence of a new term expressing a length ratio is observed. This term shows the influence not only of the electrode length but also that of the anode-to-cathode distance, and it means that in the present case the diffusion-convection reaction is actually altered by the existence of the counter-electrode. This probably arises because the velocity profile between the two surfaces of the annulus is not symmetrical, and the radius of zero momentum transfer is a function of the distance between the two surfaces.

Both equations require a linear dependence of the kinetic constant on the square root of the flow rate and on the $\frac{1}{4}$ th power of the electrode height.

The temperature coefficient of ionic mass transfer in flowing cells

As discussed elsewhere^{9,10} and as can be deduced from (1) for each particular case, the experimental heat of activation of a transport phenomenon is a complex quantity depending on the heats of activation of diffusion and momentum-transfer processes.

We notice that the heat of activation for the electrodeposition of copper ions on both tubular and annular electrodes are approximately the same, which is a quite reasonable result considering that the kinetic equations for the ionic transfer of the two cells exhibits the same dependence on the diffusion coefficient of the reacting species and on the viscosity of the solution. From (3), the relationship between the experimental heat of activation E_T , and the heats of activation for the diffusion process, E_D , and for the momentum-transfer process associated with viscosity, E_v , is

$$E_T = \frac{2}{3}E_D + \frac{1}{3}E_v \quad (9)$$

Previously we have observed¹¹ that the experimental heat of activation for rotating cylindrical electrodes with turbulent flow can be confounded with the heat of activation for diffusion; δ_N is apparently independent of temperature, as predicted by the Nernst theory¹² of the diffusion layer. For that case, the coincidence is due to a compensation of the temperature-dependent terms, because since D and ν depend inversely on T , and have the same exponent on the kinetic equation, their effects cancel out.

The temperature coefficient of the diffusion constant for copper ion in copper-sulphate-sulphuric-acid solution gives an activation energy for diffusion $E_D = 5100 \pm 400$ cal/mole.

From data obtained in our laboratory, the viscosity dependence with temperature yields $E_v = 4200 \pm 100$ cal/mole. E_T obtained with these values of E_D and E_v substituted in (9) is 4100 ± 300 cal/mole, almost within the limits of the experimental value of E_T , 4800 ± 200 cal/mole. Consequently the rate equation satisfies the energy requirements.

Finally, the heat of activation is also independent of the flow rate, as would be expected if the same flow conditions and kinetic equations for mass transfer are obeyed in the region investigated.

Current/voltage curves and concentration polarization for the ferro-ferricyanide couple

Considering (6), the dependence of k on the flow rate and on the electrode height suggests the possibility of increasing the rate of the ionic mass transfer by suitably changing both variables. Thus, a situation could be achieved in which the shape of the current/voltage curves is clearly different from that predicted by pure concentration polarization. For a redox reaction such as that of the ferro-ferricyanide couple, the concentration polarization is given by

$$\Delta E_c = \frac{2.3 RT}{ZF} \log \frac{(1 \pm I/I_c)}{(1 \mp I/I_a)} \quad (10)$$

where I_c and I_a are the cathodic and anodic limiting current densities respectively.

In Fig. 13, current/voltage curves for the ferro-ferricyanide couple under different experimental conditions are plotted according to (10). The overpotentials of the working electrode measured against the reference electrode have been suitably corrected for ohmic drop in the cell. The results give a straight line with slope $2.3 RT/F$, and it can be concluded that the redox reaction comes close to thermodynamic reversibility.

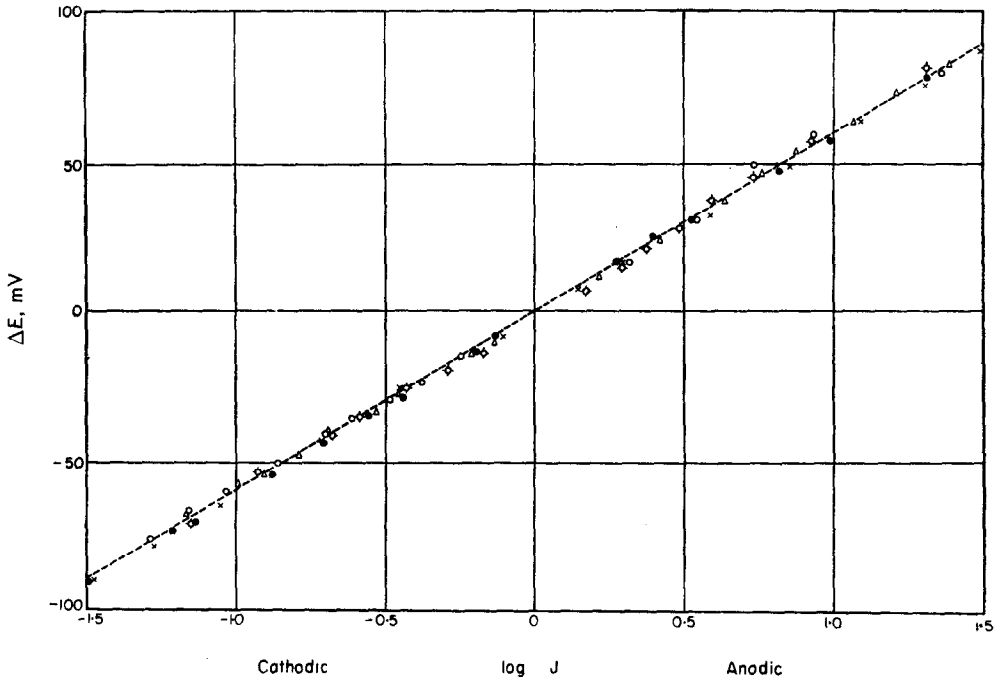


FIG. 13. Test of eq. (10).

Low velocities and electrode 1.

- : C-47 and A-19; ○: C-41 and A-45; ×: C-48 and A-49;
- △: C-42 and A-54; ◐: C-45 and A-55.

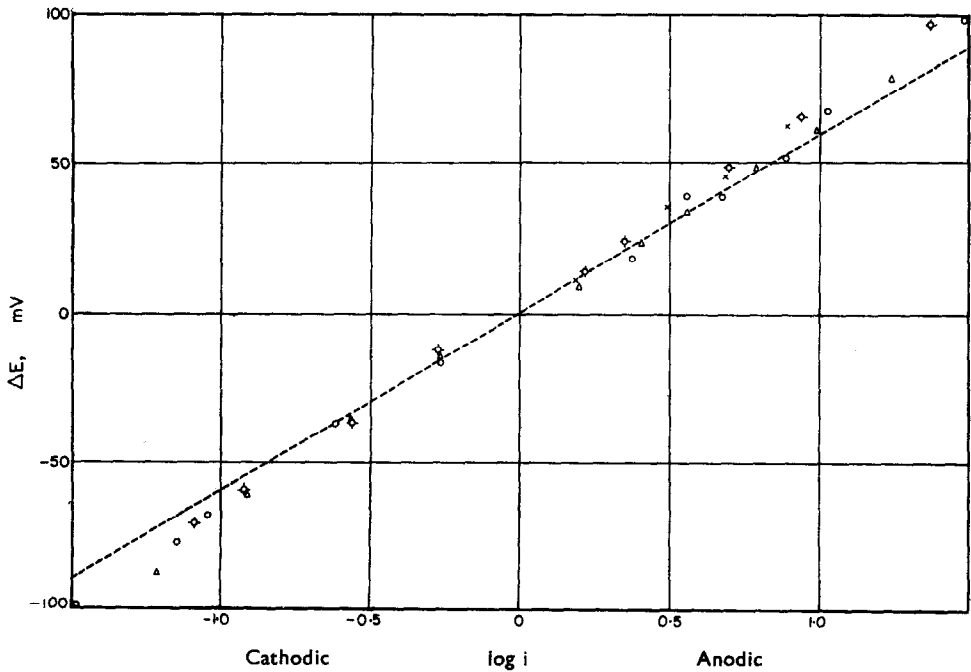


FIG. 14. Test of eq. (10).

High velocities and electrode 7.

- : C-90 and A-95; ◐: C-92 and A-98; △: C-93 and A-96; ×: A-99.

Nevertheless, a deviation from (10) is observed for the same system at the highest flow rate and the smallest electrode height employed in the present work. Fig. 14 shows a departure indicating a larger polarization than that predicted if concentration polarization alone is involved. Therefore, as Petrocelli¹³ has shown for a redox electrode, under such experimental conditions chemical polarization is becoming relatively significant.

Acknowledgements—We thank Prof. Dr. H. J. Schumacher for his interest in this work. The present work was supported with funds and a fellowship (J. C. B.) by the Consejo Nacional de Investigaciones Científicas y Técnicas of Argentina.

REFERENCES

1. J. C. BAZÁN and A. J. ARVÍA, *Electrochim. Acta* **9**, 17 (1964).
2. C. S. LIN, E. B. DENTON, H. S. GASKILL and L. G. PUTNAM, *Industr. Engng Chem.* **43**, 2136 (1951).
3. M. EISENBERG, C. W. TOBIAS and C. R. WILKE, *Trans. Electrochem. Soc.* **101**, 306 (1954).
4. A. R. GORDON and A. COLE, *J. Phys. Chem.* **40**, 733 (1936).
5. B. LEVICH, *Disc. Faraday Soc.* **1**, 37 (1947).
6. J. JORDAN and R. A. JAVICK, *J. Amer. Chem. Soc.* **80**, 1264 (1958).
7. A. RIUS, J. LLOPIS and S. POLO, *An. Fis. Quim.* **45**, 1039 (1949).
8. P. LÉVÊQUE, *J. Chim. Phys.* **49**, 266 (1952).
9. L. L. BIRCUMSHAW and A. C. RIDDIFORD, *Quart. Rev. Chem. Soc., Lond.* **6**, 157 (1952).
10. B. LEVICH, *Physicochemical Hydrodynamics*. Prentice-Hall, Englewood, N.J. (1962).
11. A. J. ARVÍA and J. S. W. CARROZZA, *Electrochim. Acta* **7**, 65 (1962).
12. W. NERNST, *Z. phys. Chem.* **47**, 53 (1904).
13. J. V. PETROCELLI, *Trans. Electrochem. Soc.* **98**, 187 (1951).